

1 Supplementary Materials

2 Estimating Rangeland Forage Production Using 3 Remote Sensing Data from a Small Unmanned Aerial 4 System (sUAS) and PlanetScope Satellite

5 Han Liu^{1*}, Randy Dahlgren¹, Royce Larsen³, Scott Devine¹, Leslie Roche², Anthony O' Geen¹,
6 Andy Wong¹, Sarah Covello³, and Yufang Jin¹

7 ¹ Department of Land, Air and Water Resources, University of California, Davis, CA, USA

8 ² Department of Plant Science, University of California, Davis, CA 95616-8627, USA

9 ³ University of California Cooperative Extension, San Luis Obispo, CA, USA

10
11 * Correspondence: haxliu@ucdavis.edu

12 1. Illumination Correction

13 We applied the C model to correct the illumination effects embedded in our sUAS data:

$$14 L_c(\lambda) = L_o(\lambda)(\cos(Z) + c(\lambda))/(IC + c(\lambda)) \dots \dots (1)$$

$$15 c = b/a \dots \dots (2)$$

$$16 L_o(\lambda) = a(\lambda) \cdot IC + b(\lambda) \dots \dots (3)$$

$$17 IC = \cos(Z) \cos(S) + \sin(Z) \sin(S) \cos(\varphi_z - \varphi_s) \dots \dots (4)$$

18 Where λ represents a specific wavelength; LC is the corrected reflectance; LO is the observed
19 reflectance; and IC is a function of topographic aspect angle (φ_z , 0° = north), slope angle (S, 0° =
20 horizontal), solar zenith angle (Z), and solar azimuth angle (φ_z). The variable c is a wavelength-
21 dependent adjustment coefficient. Coefficients *a* and *b* are the slope and intercept of the linear
22 regression between IC and observed reflectance of a specific wavelength.

23 2. sUAS and PlanetScope Data Fusion

24 We applied a simplified spatial and temporal adaptive reflectance fusion model (STARFM) to
25 fuse the monthly sUAS data with the more frequent PlanetScope data to get daily NDVI maps at 30-
26 cm resolution. We predicted the daily NDVI maps using two pairs of base sUAS and PlanetScope
27 imagery available on the nearest dates before (t_{b1}) and after (t_{b2}) the prediction date (t_p) and a
28 PlanetScope imagery on the prediction date. We calculated the weights of each base imagery pair
29 based on the correlation between the base PlanetScope imagery and the PlanetScope imagery on t_p :

$$30 W_1(x, y, t_p) = \frac{\text{Corr}(P(x, y, t_p), P(x, y, t_{b1}))}{\text{Corr}(P(x, y, t_p), P(x, y, t_{b1})) + \text{Corr}(P(x, y, t_p), P(x, y, t_{b2}))} \dots \dots (6)$$

$$31 W_2 = 1 - W_1 \dots \dots (7)$$

32 Performance of the simplified STARFM was quantitatively evaluated using a leave-one-out
33 method. Within each loop, we took out one sUAS NDVI image and predicted the image using the
34 nearest neighboring image pairs and the PS NDVI image taken on the same day. Figure S2 shows the
35 observed and predicted NDVI image on 6 April 2017 and their difference. The difference image
36 showed good agreement for the majority of the study area. The 6 April 2017 NDVI image was
37 predicted using images acquired on 17 March 2017, before peak growth, and 30 April 2017, after peak
38 growth. NDVI drops quickly after peak growth, which agrees with the non-linear shape in the scatter
39 plot of observed versus predicted NDVI on 6 April 2017 and 30 April 2017 (Fig. S3b). Meanwhile,
40 points in the scatter plot of the observed and predicted NDVI on 6 April 2017 fall close to the X=Y
41 line, indicating the simplified STARFM algorithm captured and adjusted phenological changes
42 happening between the base and predicted images.

43 3. Phenological Date Identification

44 We applied a logistic simulation over the fused NDVI time series to extract key phenological
45 information, including the green-up day and the peak biomass day:

$$46 \quad y(t) = \frac{c}{1+e^{a+bt}} + d \dots \dots (8)$$

47 Where t is the day of the year; $y(t)$ is the NDVI value at time t ; a and b are parameters to be
48 simulated; $c+d$ is the maximum NDVI value of the growing season; and d is the background NDVI
49 value. We identified the green-up day as the day when the rate of curvature change in the simulated
50 logistic function exhibits a local maximum. The peak biomass day was set as the day when NDVI
51 reaches its maximum.

52 4. Bucket Model for Deriving Daily Soil Moisture

53 The bucket model calculates the daily soil moisture (SM) using the SM on the previous day,
54 potential evapotranspiration (ET) of the day, and precipitation for the day:

$$55 \quad SM(x, y, t) = SM(x, y, t - 1) - (PET(x, y, t) - PPT(x, y, t)) * RDR$$

$$56 \quad \text{when } PPT(x, y, t) < PET(x, y, t) \dots \dots (8)$$

$$57 \quad SM(x, y, t) = SM(x, y, t - 1) + (PPT(x, y, t) - PET(x, y, t))$$

$$58 \quad \text{when } PPT(x, y, t) \geq PET(x, y, t) \dots \dots (9)$$

59 Where PPT is total precipitation, PET is potential ET, and RDR is relative drying rate, which is a
60 function of the SM on $t-1$:

$$61 \quad RDR = \frac{1 + a}{1 + aSM(x, y, t - 1)^b} \dots \dots (10)$$

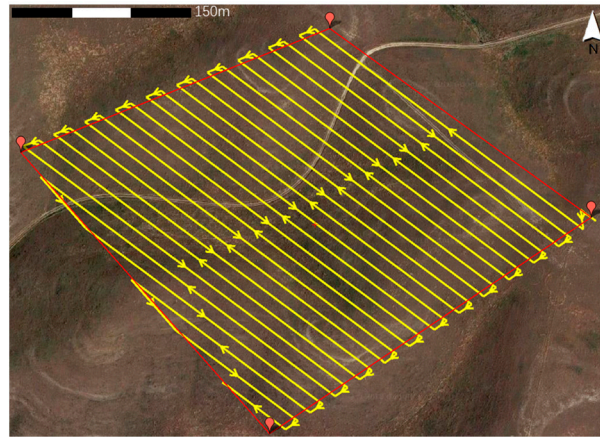
62 5. Calibration of soil moisture measurements

63 The soil moisture–biomass and soil temperature–biomass relationships were fit using a
64 univariate linear regression:

$$65 \quad y(t) = a * x(t) + b \dots \dots (11)$$

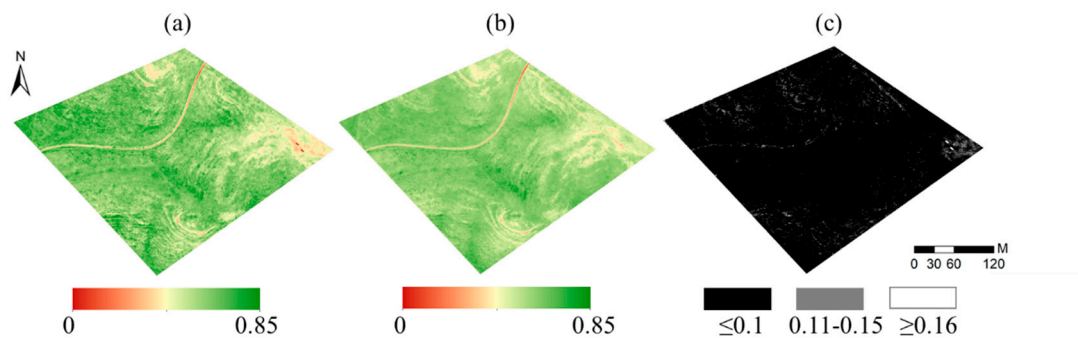
66 Where y is the measured biomass at time t and x is the Normalized Cumulated shallow (7 cm
67 depth) Soil Moisture (NCSM) or Soil Temperature (NCST) from the beginning of the growing season
68 until time t .

69 Soil moisture measurements were recalibrated using the lab-measured soil moisture content of
70 soil samples collected in April 2018. Our 5TM soil moisture sensors measure soil moisture content by
71 measuring the dielectric permittivity of the surrounding medium. The manufacturer provides a
72 universal calibration for all sensor output data, however, in some cases, plot-specific calibrations may
73 be needed as the calibration is dependent on soil texture and salinity. At our study site, we observed
74 higher sensor soil moisture measurements from an uphill south-facing slope position (point 8) than
75 a near valley position (point 13); however, in theory, soil on south-facing slopes should be drier than
76 that in the valley. We also found lower soil moisture measurements at point 8 than at point 13 from
77 an in-lab soil moisture analysis. Further lab analysis results showed while both positions have non-
78 saline soils, point 8 had silt loam texture whereas point 13 had a loam texture. We suspect that sensor
79 soil moisture measurements were affected by soil texture among different topographic positions. Our
80 recalibration assumed that the error brought by soil texture does not change throughout the growing
81 season. Based on actual soil moisture measurements from the lab, we performed a one-point
82 adjustment to all sensor soil moisture measurements, where we calculated the error using the lab
83 measurement and sensor measurement from the same day and applied the recalibration to all the
84 sensor measurements over the growing season.



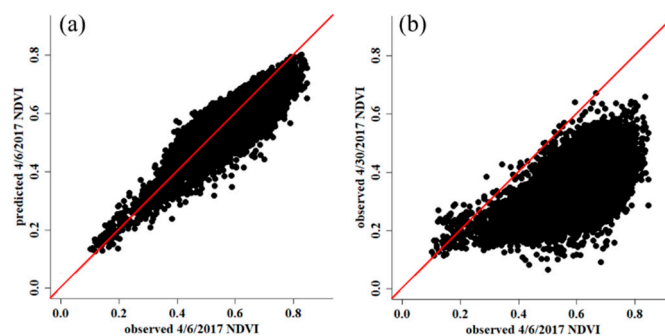
85

86 **Figure S1:** sUAS flight plan for collecting monthly aerial imagery, with a side and overlap of 85%,
 87 flying speed of 7 m/s, and fixed pre-designed flying lines (yellow) paralleled with the site boundary
 88 (red).



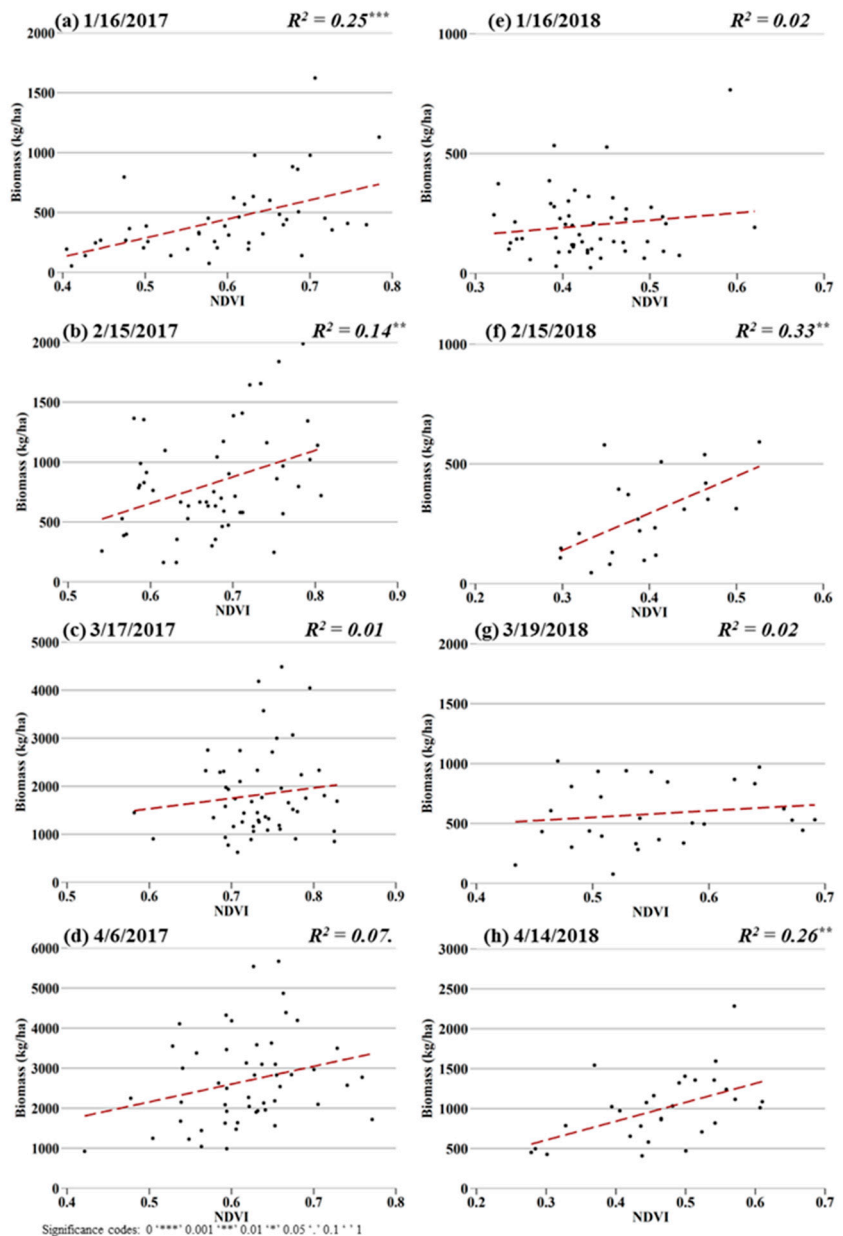
89

90 **Figure S2:** Observed NDVI image on 6 April 2017 and predicted NDVI image on 6 April 2017 based
 91 on 17 March 2017 and 30 April 2017 NDVI; the corresponding absolute difference image (c) shows
 92 very good agreement. Note areas with larger disagreements (white color) in (c) are locations where
 93 we launched the sUAS and parked fieldwork vehicles.



94

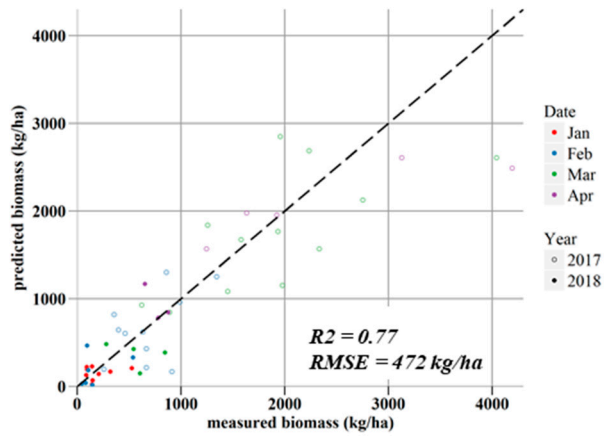
95 **Figure S3:** Scatter plot (N=10000) of (a) observed versus predicted NDVI on 6 April 2017 shows a
 96 better fit to the X=Y line (in red) than the scatter plot of (b) observed NDVI on 6 April 2017 and 30
 97 April 2017, indicating that the simplified STARFM algorithm captures some phenology changes from
 98 6 April 2017 to 30 April 2017.



99

100 **Figure S4:** Scatterplots of instantaneous sUAS NDVI and measured biomass on the eight flight dates. Each
 101 data point represents a single ground sampling point on a specific day.

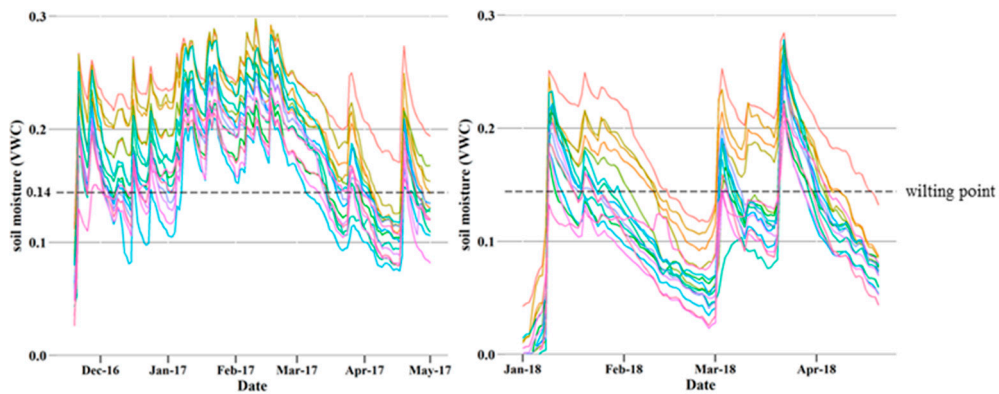
102



103

104 **Figure S5:** Scatterplot of Model III predicted biomass versus measured biomass. Each point in the
 105 plots represents a pair of predicted versus observed biomass from the validation dataset (N=50).

106



107

108 **Figure S6:** Calibrated soil moisture time series for the 2017 and 2018 growing seasons. The time series
 109 reflect the different precipitation regimes in the two growing season. The 16 soil locations are assigned
 110 different colors. Soil moisture was higher than the wilting point most of the time during the 2017
 111 growing season.

112

113

114